## SUPPLEMENTAL RESULTS AND METHODS

# Coupling of Receptor Conformation and Ligand Orientation Determine Graded Activity

**John B. Bruning[1]*, Alex A. Parent[2]*, German Gil[1], Min Zhao[1], Jason Nowak[1], Margaret C. Pace[3], Carolyn L. Smith[3], Pavel V. Afonine[4], Paul D. Adams[4], John A. Katzenellenbogen[2], and Kendall W. Nettles[1]**

[1]Department of Cancer Biology, The Scripps Research Institute, Scripps Florida, 130 Scripps Way, Jupiter, FL, 33458, USA

[2]Department of Chemistry, University of Illinois, Urbana, IL 61801, USA

[3]Department of Molecular and Cellular Biology, Baylor College of Medicine, One Baylor Plaza, Houston, TX 77030, USA

[4]Lawrence Berkeley National Laboratory, BLDG 64R0121, 1 Cyclotron Road, Berkeley, CA 94720, USA.

*Contributed equally

Correspondence: Kendall W. Nettles, Tel 561-288-3209, knettles@scripps.edu

# SUPPLEMENTAL RESULTS

**WAY-169916 bound to the inactive conformation of ERα**

In the unconstrained conformer, ligand orientations #2 and #3 display optimal stacking interactions between the indazole moieties (**Supplemental Figures 3a and 4a**). Relative to the ligand position in the agonist conformation structure (orientation #1), orientation #2 maintains the hydrogen bonding pattern with the phenol, but the $CF_3$ group is shifted by 4.5 Å away from the *C*-terminus of helix 11 and towards the *N*-terminus of helix 3 (**Supplemental Figure 4b**). For orientation #3 (**Supplemental Figure 4c**), the $CF_3$ group is positioned near H525 in helix 11, as seen with ligand orientation #1 in the agonist conformation structure. However, the phenol group does not form the canonical hydrogen bond with E353 and R394, seen with all other ER ligands to date, but rather extends out of the pocket between helices 3 and 11, where it clashes with the agonist positioning of helix 12 (**Supplemental Figure 4c**). Here the phenol group forms a hydrogen bond with D351, similar to the interactions seen with most ER antagonist basic side chains. The allyl side group of WAY-169916 is then oriented towards helix 11, inducing a dramatic shift in helix 11 of 3.5 Å from the position seen with the agonist conformer. Both the presence of a second ligand in the pocket, and the specific binding interactions of ligand orientations #2 and #3 define novel binding epitopes for the steroid hormone receptors. A key feature of these alternate binding modes (#2 and #3) is the role of the allyl side group of WAY-169916 in stabilizing specific ligand orientations.

The partially constrained conformer shows electron density in the ligand-binding pocket that is different from the unconstrained chain. In contrast to the non-overlapping ligands in the unconstrained conformer, the electron density suggested two overlapping ligand orientations, including #2, and yet another novel binding mode for the ligand, orientation #4 (**Supplemental Figures 3b and 4d**). Compared to ligand orientation #1, orientation #4 shows the indazole scaffold flipped 180°, maintaining the interaction of the $CF_3$ group with helix 11 and the hydrogen bonding pattern of the phenol (**Supplemental Figure 4e**). This flip positions the allyl side group of the ligand where it clashes with the agonist conformation of helix 11 L525, inducing the shift in the position of helix 11 that also disrupts the active conformation of helix 12.

The last rounds of refinement revealed additional electron density indicating that that ligand orientation #3 also binds to the partially constrained conformer (**Supplemental Figure 3c**). To define their relative occupancies, we implemented a new method for group occupancy refinement in the PHENIX software, allowing the occupancy of orientation #4 to be simultaneously grouped with orientation #2 or with #3. In the final model, orientation #4 has 28-30% occupancy, while the other orientations have occupancies of 70-72% in the partially constrained conformers (**Supplemental Figure 3d**).

To validate the modeled ligand orientations, we deleted all ligands from the final model, and re-refined the structure with a bias removal protocol (see Methods). This ensures that the omit maps are not biased by the previous refinement with the ligands. The omit maps clearly support the presence of ligand orientation #4 in the constrained conformer, and not in the unconstrained conformer (**Supplemental Figure 3e**). We conclude that the partially constrained conformation of ERα allows trapping of a ligand binding orientation that is not apparent in the unconstrained conformation.

**Supplemental Table 1 Data collection and refinement statistics**

| **Mutation**<br>**Compound** | **537S**<br>**WAY** | **372R/536S**<br>**WAY** | **536S**<br>**Raloxifene** | **372R/536S**<br>**Benzyl** | **372R/536S-**<br>**Methylbutenyl** |
|---|---|---|---|---|---|
| **Data collection** | | | | | |
| Space group | P1 21 1 | P 1 | C2 | P1 | P1 |
| Cell dimensions | | | | | |
| *a*, *b*, *c* (Å) | 55.81, 82.03, 58.52 | 52.90, 59.06, 93.76 | 101.59, 58.10, 87.95 | 53.70, 58.57, 93.46 | 53.56, 58.48, 93.32 |
| $\alpha, \beta, \gamma$ (°) | 90.00, 109.04, 90.00 | 86.64, 74.64, 63.43 | 90.00, 102.66, 90.00 | 80.40, 74.85, 62.79 | 85.88, 74.75, 62.76 |
| Resolution (Å) | 15.0-1.8 | 20-2.3 | 15-1.70 | 38.2-2.28 | 38.15-2.30 |
| $R_{sym}$ or $R_{merge}$ | 0.046(0.176) | 0.081(0.468) | 0.066(0.303) | 0.053(0.23) | 0.176(0.312) |
| $I / \sigma I$ | 23.10(6.57) | 14.86(1.96) | 24.34(5.55) | 19.0 (3.0) | 21.12(2.83) |
| Completeness (%) | 95.4(92.1) | 91.42(63) | 99.9(99.0) | 88.8 (63) | 87.8 (65) |
| Redundancy | 4.7(3.4) | 3.2(2.2) | 6.7(4.5) | 1.9(1.6) | 3.6(3.0) |
| | | | | | |
| **Refinement** | | | | | |
| Resolution (Å) | 10-1.8 | 15-2.30 | 15-1.70 | 45.0-2.28 | 38.15-2.30 |
| No. reflections | 43998 | 39541 | 55230 | 39248 | 38048 |
| $R_{work}$ / $R_{free}$ | 22.09/17.79 | 24.91/20.48 | 21.58/18.25 | 22.81/18.12 | 24.98/19.61 |
| No. atoms | | | | | |
| Protein | 3894 | 7017 | 3709 | 7434 | 7373 |
| Ligand/ion | 48 | 240 | 68 | 112 | 104 |
| Water | 422 | 217 | 300 | 267 | 311 |
| *B*-factors | | | | | |
| Protein | 35.9 | 69.8 | 21.6 | 49.1 | 44.3 |
| Ligand/ion | 32.4 | 50.2 | 15.5 | 46.9 | 44.0 |
| Water | 46.0 | 65.1 | 34.8 | 44.1 | 49.7 |
| R.m.s. deviations | | | | | |
| Bond lengths (Å) | 0.014 | 0.005 | 0.012 | 0.004 | 0.015 |
| Bond angles (°) | 1.489 | 0.727 | 1.464 | 0.866 | 1.656 |

*Highest-resolution shell is shown in parentheses.

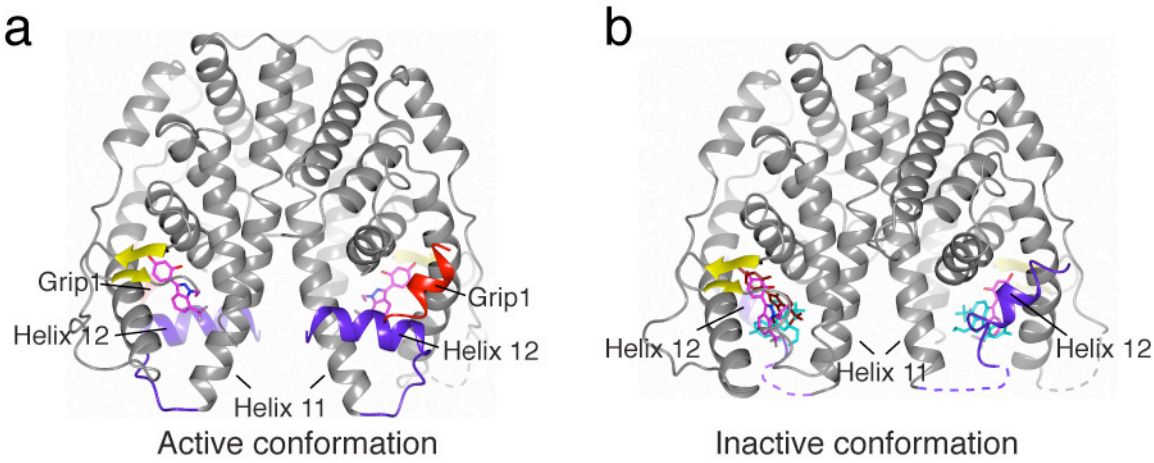


**Supplemental Figure 1. Structures of WAY-169916 bound to ERα ligand binding domain in active or inactive conformations.**

(**a**) Ribbon diagram of WAY-169916 bound to dimeric ERα in the active conformation. Helix 12 is colored blue, forming one side of the coactivator-binding site. The bound Grip1 coactivator peptides are colored red. Dashed lines indicate loops that are disordered.

(**b**) WAY-169916 bound to dimeric ERα in the inactive conformation, showing binding of the ligand in multiple orientations. Helix 12 is colored blue, and binds in the coactivator-binding groove. Dashed lines indicate loops that are disordered.

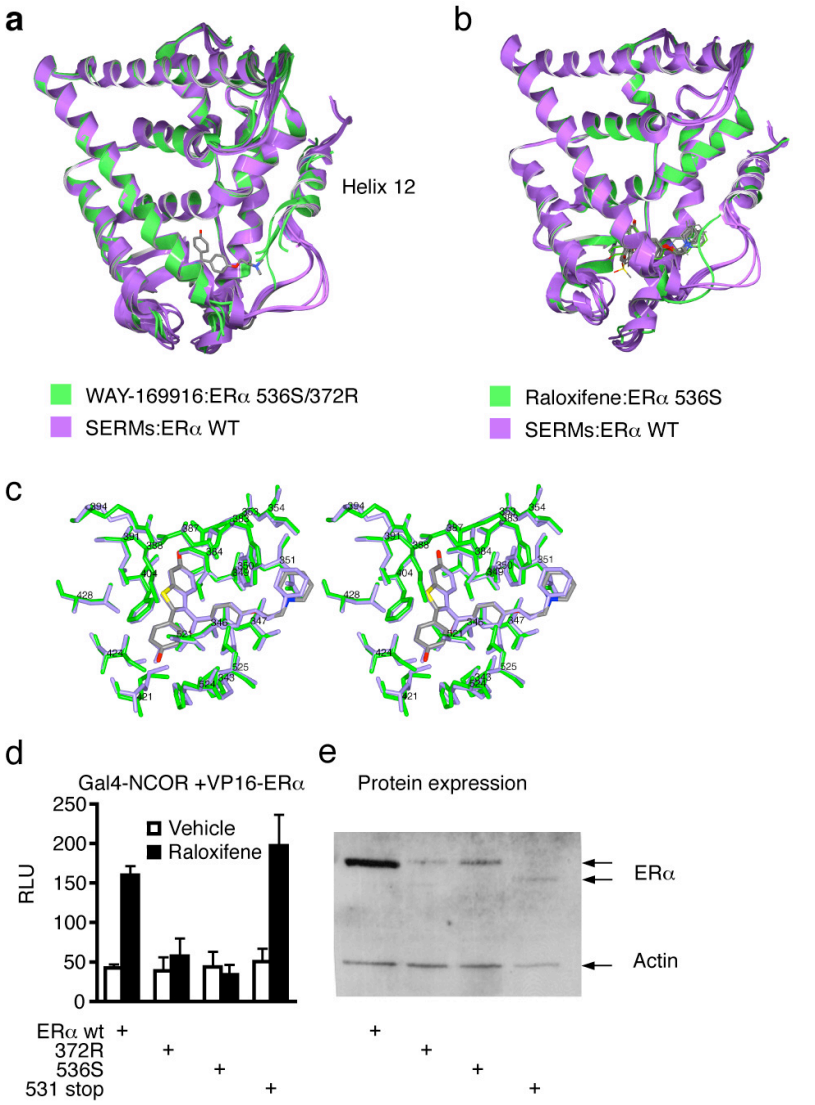


**Supplemental Figure 2. Characterization of inactive conformation mutants of ERα**

(**a**) The four monomers of the WAY-69916 ERα L372R/L536S structure are shown as green ribbons, and superimposed with eleven published structures of ERα showing the antagonist conformation of helix 12, colored purple. Tamoxifen is shown as a stick.

(**b**) The structure of Raloxifene bound to the mutant ERα 536S (green) was superimposed with eleven published antagonist ERα structures, colored purple, and show as ribbons. These include PDB codes 1UOM, 1XP6, 1ERR, 1YIM, 1XP9, 2AYR, 1XPC, 1XQC, 1XP1, 1UIZ, and 3ERT.

(**c**) The structure of Raloxifene bound to the mutant ERα was superimposed with the wild type ERα Raloxifene structure, colored purple (PDB code 1ERR). Shown is a stereo view of amino acids that contact the ligand. Residues in the mutant structure are colored green, and the ligand is colored gray.

(**d**) A mammalian two-hybrid assay was used to examine the raloxifene dependent interaction between wild type VP16-ERα or the VP16-ERα-372R, VP16-ERα-536S, or VP16-ERα-531stop mutants and the Gal4-NCOR corepressor using a Gal4-luciferase reporter. Data represent mean + SEM. RLU, relative light units.

(**e**) A western blot shows the relative levels of wild-type VP16-ERα versus the indicated mutant VP16-ERα constructs in the transfected cells.

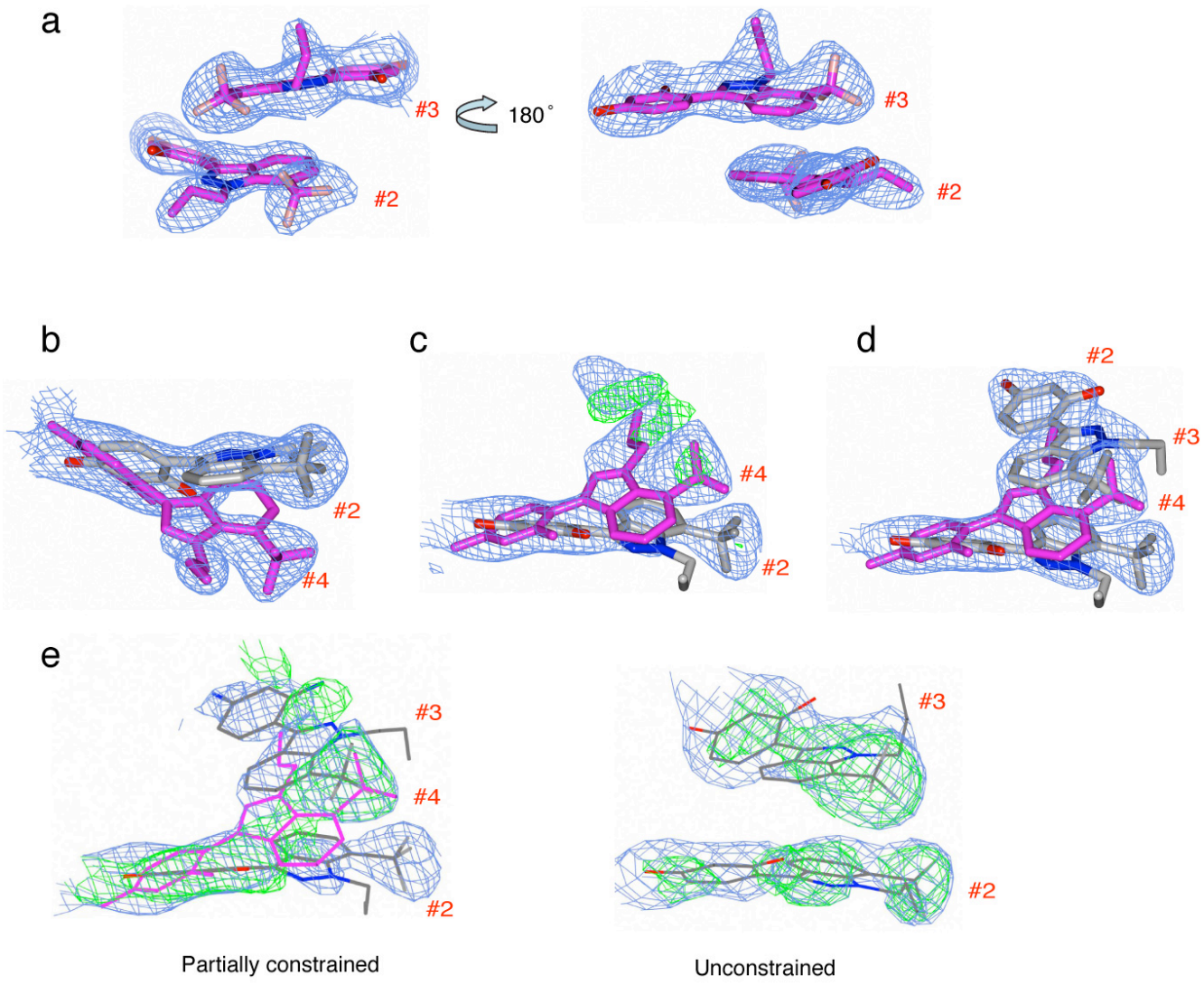


**Supplemental Figure 3. Electron density maps for WAY-166916 bound to the inactive conformation structure of ERα**

(**a**) Shown are the two WAY-169916 orientations #2 and #3 from the unconstrained conformer of the inactive conformation structure of ERα. The 2Fo-Fc map is contoured to 1 **σ.**

(**b**) A 2Fo-Fc electron density map after initial docking of the ligands in the partially constrained inactive conformer, contoured to 1.0 σ**.** Shown are ligand orientation #2 (gray), and a partially overlapping orientation #4 (magenta).

(**c**) Electron density maps are shown after further refinement of the structure with ligand orientations #2 and #4 bound to the partially constrained conformer. The 2Fo-Fc map is colored blue, and contoured to 1 σ, while an Fo-Fc difference map is colored green and contoured to 3 σ. Both maps suggest missing atoms, corresponding to the shape of ligand orientation #3.

(**d**) A 2Fo-Fc electron density map, contoured to 1 σ, after docking of ligand orientation #3 and group constrained occupancy refinement of the ligands, described in Experimental Procedures.

(**e**) 2Fo-Fc (1 σ) and Fo-Fc (3 σ) ligand omit maps were calculated after deleting the ligands from the final model and performing a bias removal refinement protocol, which is described in the Experimental Procedures. Both maps support the presence of ligand orientation #4 only in the partially constrained conformer. Ligand orientation #4 is colored magenta, and the others CPK.

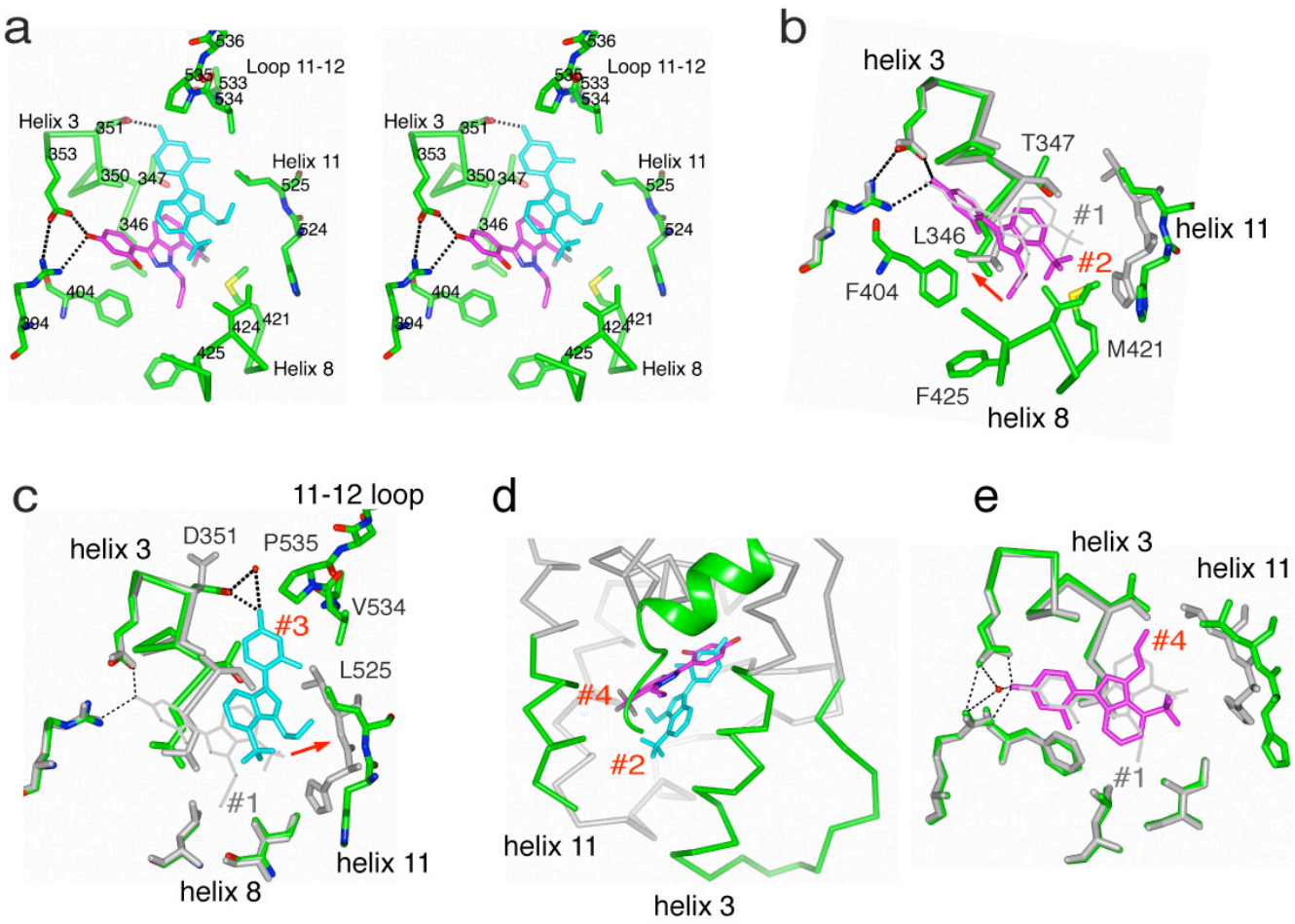


**Supplemental Figure 4**

(**a**) A stereo view of ligand orientations #2 (magenta) and #3 (blue). Selected amino acids that contact the ligands are numbered, and colored green.

(**b**) Comparison of ligand orientation #1 in the active conformer (gray) with ligand orientation #2 (green protein and magenta compound) in the unconstrained conformer. The red arrow denotes the shift in helix 3 induced by the ligand. Selected amino acids that directly interact with the ligand are shown.

(**c**) Same as (**e**), but showing ligand orientation #3 and selected interacting side-chains.

(**d**) A c-$\alpha$ trace of the partially constrained conformer is shown, with Helix 12 displayed as ribbon. Overlapping orientations #2 and #4 are colored cyan and magenta, respectively.

(**e**) Comparison of ligand orientation #1 in the active conformer (gray) with ligand orientation #4 in the partially constrained conformer, with the protein colored green and the compound colored magenta.

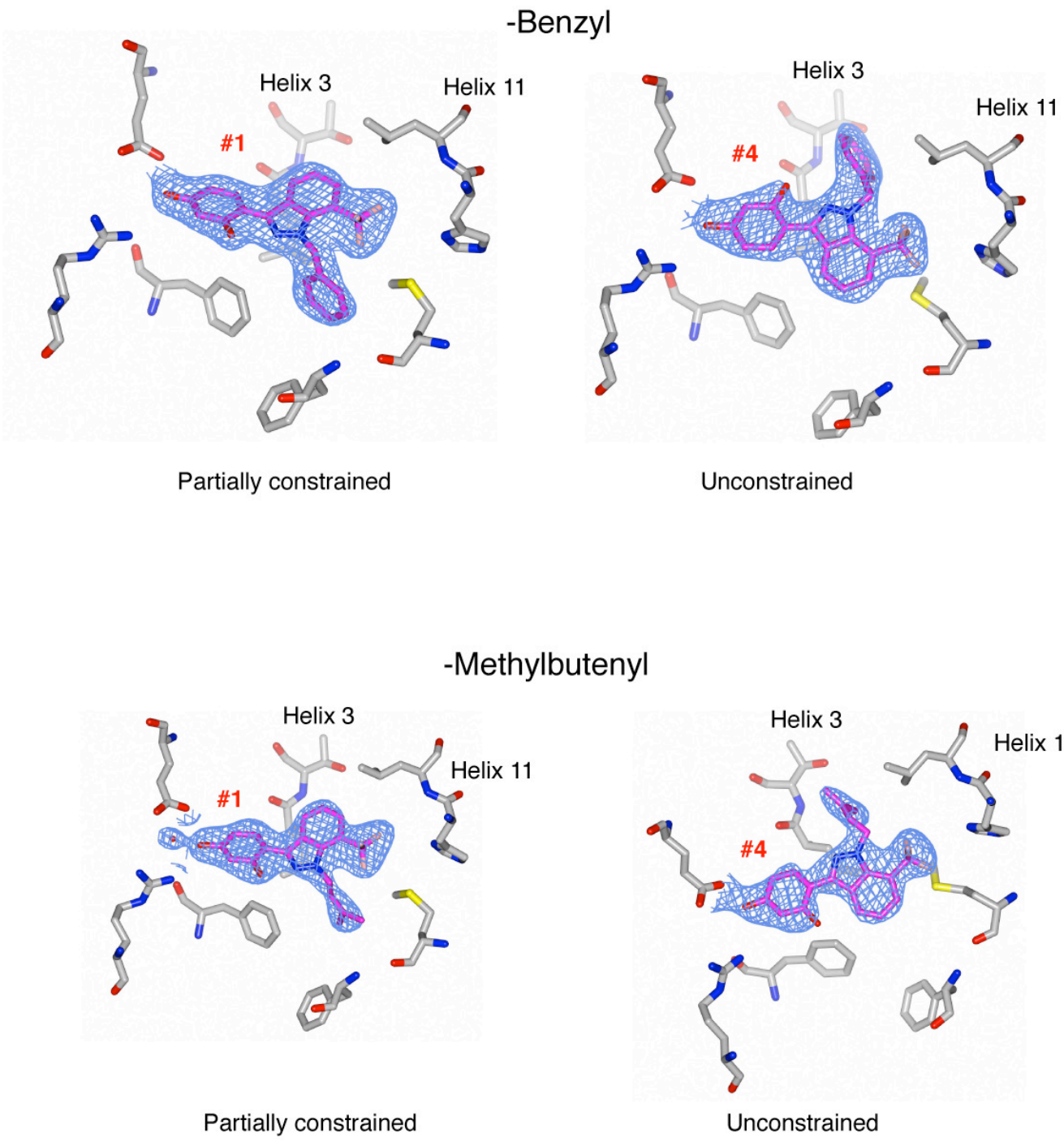


**Supplemental Figure 5. Electron density for WAY-169916 derivatives bound to inactive conformation ERα 372R/536S**

The benzyl and methylbutenyl derivatives are shown in both conformers of their inactive conformation structures, with the 2Fo-Fc maps contoured to 1.2 σ.

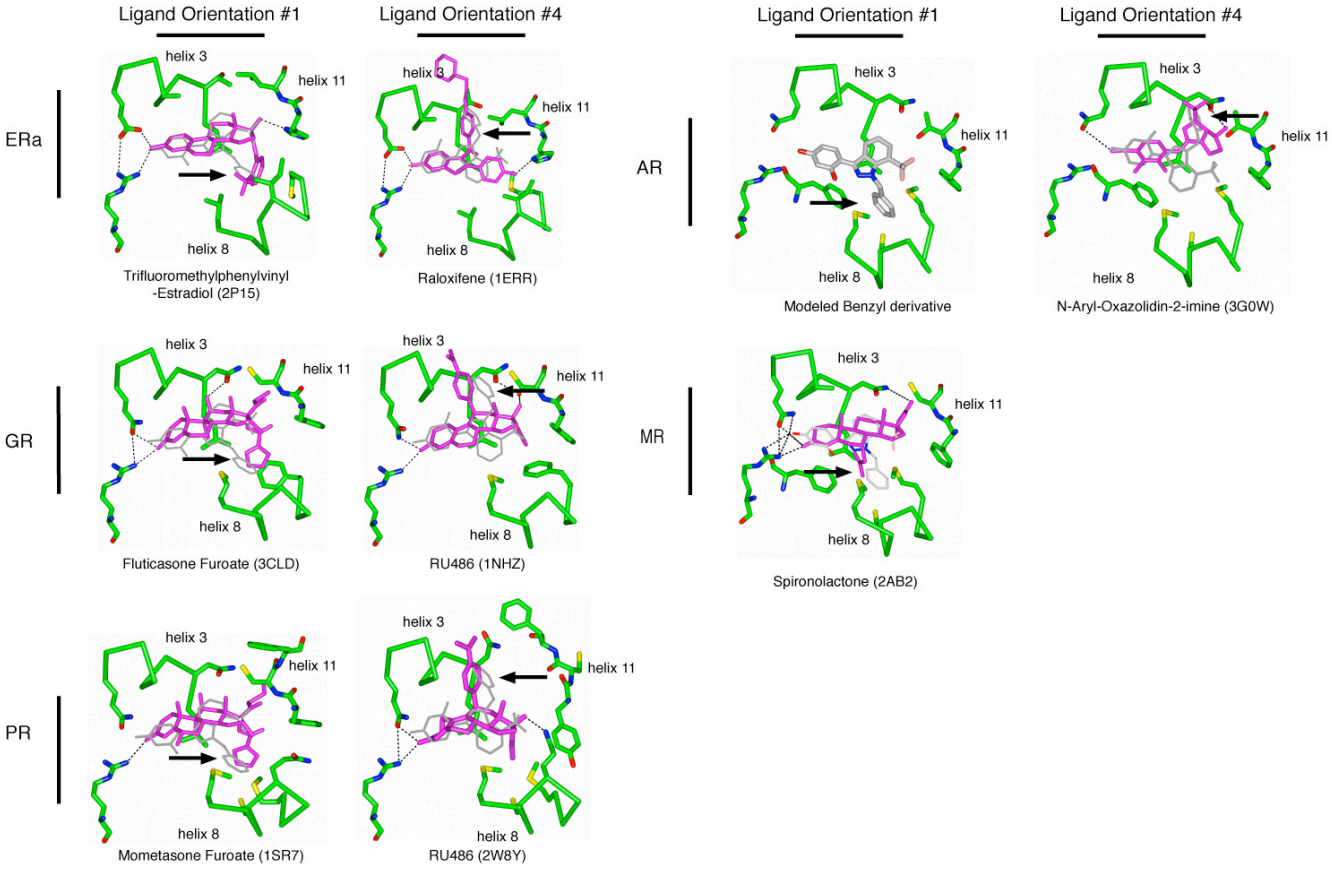


**Supplemental Figure 6. Ligand orientations in the steroid receptor family**

The benzyl derivative ERα structure was superimposed with the structure indicated by the pdb code in parentheses. The benzyl compound is shown as thin bonds, while the superimposed structure is colored green, with the bound ligand colored magenta. The arrows highlight side groups that occupy the same binding epitope as the benzyl in either orientation #1 or #4. With AR, there is no structure of a ligand in orientation #1, but the pocket formed by helix 8 is highly conserved. Docking of the benzyl derivative in orientation #1 onto AR (pdb code:3G0W) shows that the benzyl group forms close VDW interactions with the surrounding residues, and no clashes.

# SUPPLEMENTAL METHODS

## SYNTHETIC DETAILS

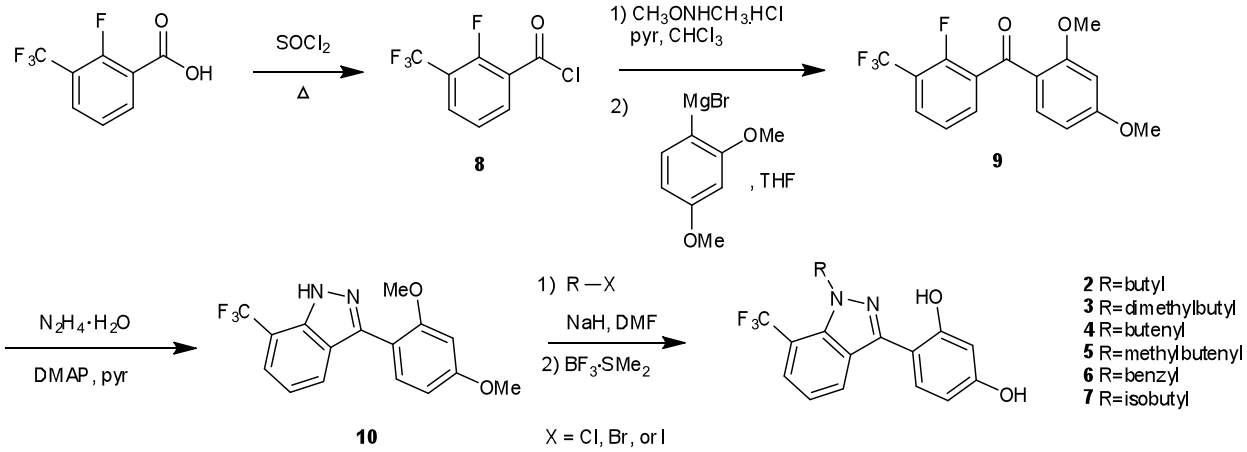


**General Synthetic Methods.** All reagents were used as purchased except where noted. THF, $CH_2Cl_2$, and DMF used in reactions were dried using a solvent delivery system (neutral alumina column). Solvents used for extraction and flash chromatography were reagent or Ultima grade purchased from either Aldrich or Fisher Scientific. All reactions were run under a dry $N_2$ atmosphere except where noted. Flash column chromatography was performed on Silica P Flash Silica Gel (40-64 μM, 60Å) from SiliCycle®. $^1$HNMR and $^{13}$CNMR spectra were obtained on 500 MHz Varian® FT-NMR spectrometers. High resolution mass spectra were obtained using electrospray ionization on either a Micromass Q-ToF Ultima or Waters Quattro instrument. The WAY-169916 used for the biological and crystallographic studies described in this paper was synthesized in house and had spectrographic characterization identical to literature values (Mosyak et al., 2006; Steffan et al., 2004). Except where noted, the synthetic pathway for all derivatives closely follows that previously described for the synthesis of WAY-169916.

**2-fluoro-3-(trifluoromethyl)benzoyl chloride (8).** 2-fluoro-3-(trifluoromethyl)benzoic acid (5.0 g, 24 mmol) was dissolved in 8.8 ml $SOCl_2$ (120 mmol) and heated at reflux for 2 h. The excess thionyl chloride was removed *in vacuo*. To the resulting oil, two sequential aliquots of benzene were added with subsequent removal of solvent by rotary evaporator after each addition. The oil was placed on a high vacuum pump over night and used without further purification (3.96 g, 73%). $^1$H NMR (500 MHz, $CDCl_3$) δ 7.47 (t, *J*=7.93 Hz, 1 H) 7.94 (t, *J*=6.59 Hz, 1 H) 8.31 (t, *J*=7.32 Hz, 2 H). Although compound **8** was synthesized in this study, it should be noted that it is a known and commercially available substance and consequently further characterization was not pursued.

**(2,4-Dimethoxyphenyl)(2-fluoro-3-(trifluoromethyl)phenyl)methanone (9).** 2-Fluoro-3-(trifluoromethyl)benzoyl chloride **8** (3.96 g, 17.5 mmol) and N,O-dimethylhydroxylamine HCl (1.87 g, 19.2 mmol) were added to 6 mL $CHCl_3$. The reaction mixture was cooled to 0 °C and 3.11 mL (38.5

mmol) of pyridine was added dropwise with stirring. The reaction mixture was stirred at room temperature for 45 minutes, and the solvent removed *in vacuo*. The resulting residue was extracted from saturated NaCl solution three times with $CHCl_3$; the combined organic layers were then washed once with saturated NaCl and dried over anhydrous $MgSO_4$. The solvent was removed by rotary evaporator, and the resulting oil was placed on high vacuum over night. The crude Weinreb amide was subsequently dissolved in 140 mL of dry THF, and the resulting solution cooled to 0 °C. 50 mL of a 0.5 M solution of 2,4-dimethoxyphenyl magnesium bromide (25 mmol) was added, and reaction mixture was allowed to warm to room temperature. After three hours, the reaction was quenched with 50 mL of 1N aq. HCl (upon acidification the brown solution became a deep purple) and extracted twice with $Et_2O$ and once with $CH_2Cl_2$. The combined organic layers were dried over anhydrous $MgSO_4$ and the solvent removed in vacuo. The product was purified by flash column chromatography on silica eluted with 100% $CH_2Cl_2$ to give 3.76 g of **9** (64%). $^1$H NMR (500 MHz, $CDCl_3$) δ 3.62 (s, 3 H), 3.88 (s, 3 H), 6.44 (d, *J*=2.44 Hz, 1 H), 6.59 (dd, *J*=8.67, 2.32 Hz, 1 H), 7.32 (t, *J*=7.81 Hz, 1 H), 7.71 (t, *J*=6.59 Hz, 1 H), 7.77 (d, *J*=8.79 Hz, 1 H), 7.81 (t, *J*=6.23 Hz, 1 H). $^{13}$C NMR (500 MHz, $CDCl_3$) δ 55.6, 55.8, 98.5, 105.8, 121.2, 122.7 (d, *J*=272.47 Hz), 124.0, 124.1, 129.2 (dd, *J*=4.88, 1.95 Hz), 131.6 (d, *J*=13.67 Hz), 133.4, 134.3 (d, *J*=3.91 Hz), 157.8 (d, *J*=261.73 Hz), 161.4, 165.5, 189.2. HRMS (ESI$^+$) *m/z* calcd for $C_{16}H_{13}O_3F_4^+$ 329.0801, found 329.0791.

**3-(2,4-Dimethoxyphenyl)-7-(trifluoromethyl)-1H-indazole (10).** 3.51 g (10.7 mmol) of (2,4-dimethoxyphenyl)(2-fluoro-3-(trifluoromethyl)phenyl)methanone **9** and 1.31 g (10.7 mmol) of DMAP were dissolved in 30 mL of pyridine. To this solution, 6.66 mL of hydrazine hydrate (50–60% $N_2H_4$, ~107 mmol) were added dropwise with stirring. The reaction mixture was heated to 115 °C for 18 h, cooled to room temperature, and acidified with ~ 300 mL of 1N aq. HCl solution. The reaction was extracted three times with EtOAc, and the combined organic layers were washed with saturated NaCl solution and dried over anhydrous $MgSO_4$. The solvent was removed *in vacuo*, and the resulting residue purified by flash chromatography on silica (10% EtOAc in $CH_2Cl_2$) to give 3.04 g (88%) of **10**. $^1$H NMR (500 MHz, $CDCl_3$) δ 3.85 (s, 3 H), 3.92 (s, 3 H), 6.65 - 6.68 (m, 2 H), 7.24 (t, *J*=8.04 Hz, 1 H), 7.59 (d, *J*=7.72 Hz, 1 H), 7.67 (dt, *J*=7.24, 0.88 Hz, 1 H), 7.96 (d, *J*=7.93 Hz, 1 H), 10.60 (br s, 1 H). $^{13}$C NMR (500 MHz, $CDCl_3$) δ 55.8, 99.3, 105.2, 120.2, 124.5 (d, *J*=4.6 Hz), 127.0, 132.3, 161.8. HRMS (ESI$^+$) *m/z* calcd for $C_{16}H_{14}N_2O_2F_3^+$ 323.1007, found 323.0997.

**General procedure for the formation of 4-(1-alkyl-7-(trifluoromethyl)-1H-indazol-3-yl)benzene-1,3-diols (2-7)**. To 100 mg (0.31 mmol) of 3-(2,4-dimethoxyphenyl)-7-(trifluoromethyl)-1H-indazole **10** dissolved in 2 mL of DMF were added 14–30 mg of NaH (60% dispersion in mineral oil, 0.35-0.75 mmol). After stirring for 15 minutes at room temperature, 0.34–0.69 mmol of alkyl halide was added, and the reaction was stirred at 20–80 °C until complete consumption of starting material, as shown by

TLC analysis (4–24 h). The reaction was cooled to room temperature and extracted from 1N aq. HCl three times with EtOAc. The combined organic fractions were dried over $MgSO_4$ and solvent removed *in vacuo*. The resulting residue was dissolved in 1 mL $CH_2Cl_2$ and cooled to 0 °C. To this solution, 1 mL of $BF_3$•$SMe_2$ was added dropwise with stirring, immediately producing dense smoke and cloudy precipitate in the reaction mixture (Konieczny et al., 2005). The solution was allowed to warm to room temperature, stirred overnight, and quenched with MeOH. The solvent was removed *in vacuo*, and the residue purified by flash chromatography on silica (25-50% EtOAc in hexanes and/or 10% EtOAc in $CH_2Cl_2$).

**4-(1-Butyl-7-(trifluoromethyl)-1H-indazol-3-yl)benzene-1,3-diol (2)**. Followed general procedure described above using 14 mg NaH (0.35 mmol) and 47 mg (0.34 mmol) of 1-bromobutane stirred at room temperature for 6 h. Flash column eluted with 25–50% EtOAc in hexanes gave 27 mg (24%) of **2**. $^{1}$H NMR (500 MHz, $CDCl_3$) δ 0.98 (t, *J*=7.45 Hz, 3 H), 1.45 (sextet, *J*=7.57 Hz, 2 H), 1.94 (quintet, *J*=7.57 Hz, 2 H), 4.53 (t, *J*=7.57 Hz, 2 H), 5.35 (s, 1 H), 6.57 (dd, *J*=8.55, 2.44 Hz, 1 H), 6.64 (d, *J*=2.44 Hz, 1 H), 7.29 (t, *J*=7.81 Hz, 1 H), 7.83 (d, *J*=7.32 Hz, 1 H), 7.87 (d, *J*=8.55 Hz, 1 H), 8.36 (d, *J*=8.06 Hz, 1 H), 10.92 (s, 1 H). $^{13}$C NMR (500 MHz, $CDCl_3$) δ 13.9, 20.2, 32.4, 51.2 (d, *J*=3.91 Hz), 104.3, 107.6, 110.5, 120.1, 123.0, 124.0, 126.5 (d, *J*=5.86 Hz), 126.9, 128.4, 135.7, 143.8, 157.2, 157.9. HRMS (ESI$^+$) *m/z* calcd for $C_{18}H_{18}N_2O_2F_3^+$ 351.1320, found 351.1320.

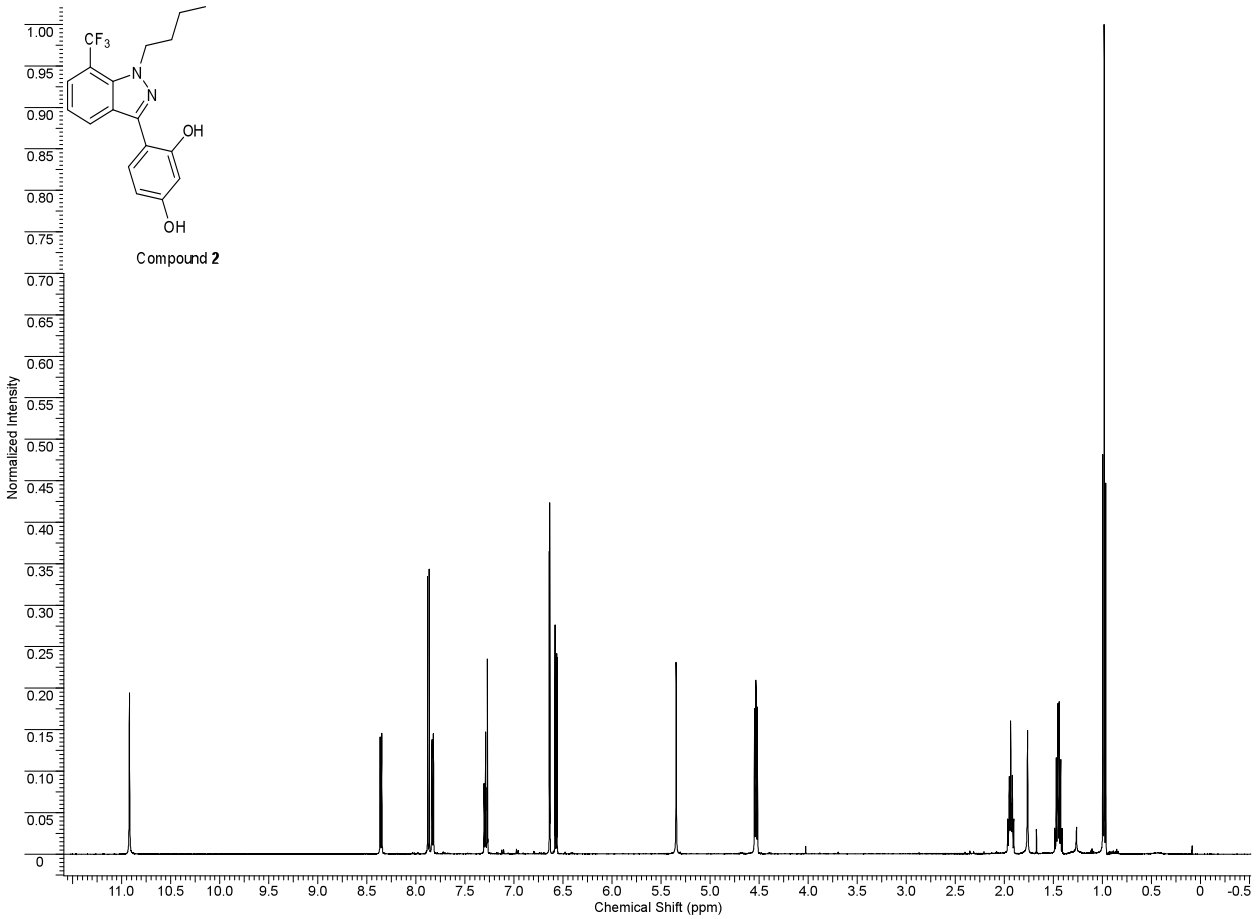


**Figure 1.** $^{1}$HNMR spectrum of compound **2**

**4-(1-(3,3-Dimethylbutyl)-7-(trifluoromethyl)-1H-indazol-3-yl)benzene-1,3-diol (3)**. Followed general procedure described above using 19 mg NaH (0.46 mmol) and 58 mg (0.46 mmol) of 1-chloro-3,3-dimethylbutane stirred at 80 °C overnight. Flash column eluted with 25–50% EtOAc in hexanes gave 12 mg (10%) of **3**. $^{1}$H NMR (500 MHz, $CDCl_3$) δ 1.05 (s, 9 H), 1.83 - 1.88 (m, 2 H), 4.54 - 4.59 (m, 2 H), 5.09 (s, 1 H), 6.56 (dd, *J*=8.55, 2.44 Hz, 1 H), 6.62 (d, *J*=2.44 Hz, 1 H), 7.29 (t, *J*=7.81 Hz, 1 H), 7.83 (d, *J*=7.32 Hz, 1 H), 7.87 (d, *J*=8.30 Hz, 1 H), 8.36 (d, *J*=8.30 Hz, 1 H), 10.85 (s, 1 H). $^{13}$C NMR (500 MHz, $CDCl_3$) δ 29.6, 30.1, 43.5, 48.5 (d, *J*=5.52 Hz), 104.2, 107.5, 110.6, 120.1, 121.8, 124.0, 125.1, 126.5 (d, *J*=6.44 Hz), 126.9, 128.5, 143.9, 157.1, 158.0. HRMS (ESI$^+$) *m/z* calcd for $C_{20}H_{22}N_2O_2F_3^+$ 379.1633, found 379.1618.

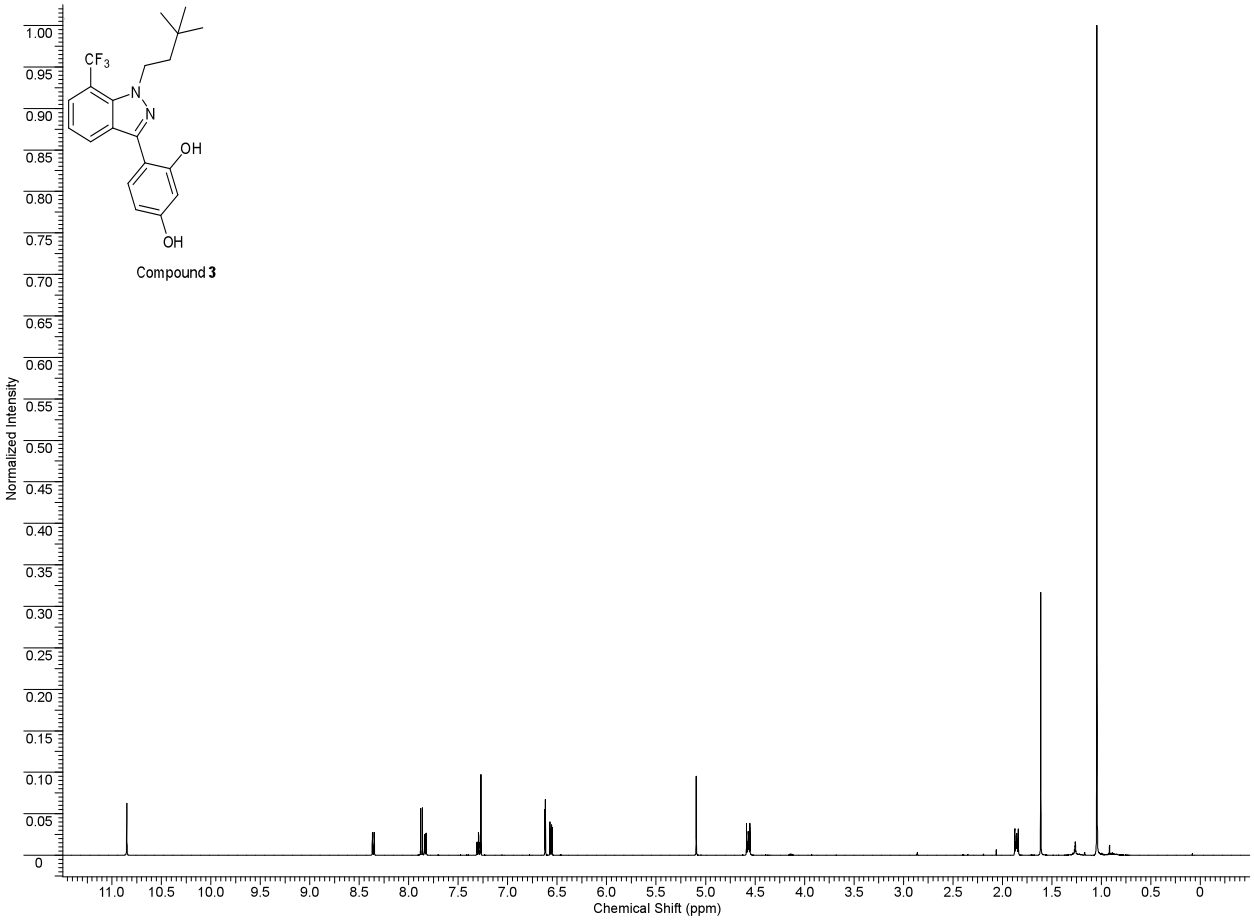


**Figure 2.** $^{1}$HNMR spectrum of compound **3**

**4-(1-(But-3-enyl)-7-(trifluoromethyl)-1H-indazol-3-yl)benzene-1,3-diol (4)**. Followed general procedure described above using 30 mg NaH (0.75 mmol) and 66 mg (0.48 mmol) of 4-bromo-1-butene stirred at room temperature for 24 h and 60 °C for 2 h. Flash column eluted with 25–50% EtOAc in hexanes gave 24 mg (22%) of **4**. $^{1}$H NMR (500 MHz, $CDCl_3$) δ 2.70 (q, *J*=7.24 Hz, 2 H), 4.61 (t, *J*=7.57 Hz, 2 H), 5.09 (dd, *J*=10.25, 1.46 Hz, 1 H), 5.14 (dq, *J*=17.09, 1.46 Hz, 1 H), 5.25 (s, 1 H), 5.83 - 5.92 (m, 1 H), 6.57 (dd, *J*=8.42, 2.56 Hz, 1 H), 6.63 (d, *J*=2.44 Hz, 1 H), 7.30 (t, *J*=7.81 Hz, 1 H), 7.84 (d, *J*=7.57 Hz, 1 H), 7.86 (d, *J*=8.30 Hz, 1 H), 8.36 (d, *J*=8.30 Hz, 1 H), 10.78 (s, 1 H). $^{13}$C NMR (500 MHz, $CDCl_3$) δ 34.5, 50.7 (d, *J*=4.88 Hz), 104.3, 107.6, 110.5, 117.9, 120.3, 124.1, 126.5 (d, *J*=6.84 Hz), 127.0, 128.5, 134.2, 144.0, 157.3, 157.9. HRMS (ESI$^+$) *m/z* calcd for $C_{18}H_{16}N_2O_2F_3^+$ 349.1164, found 349.1150.

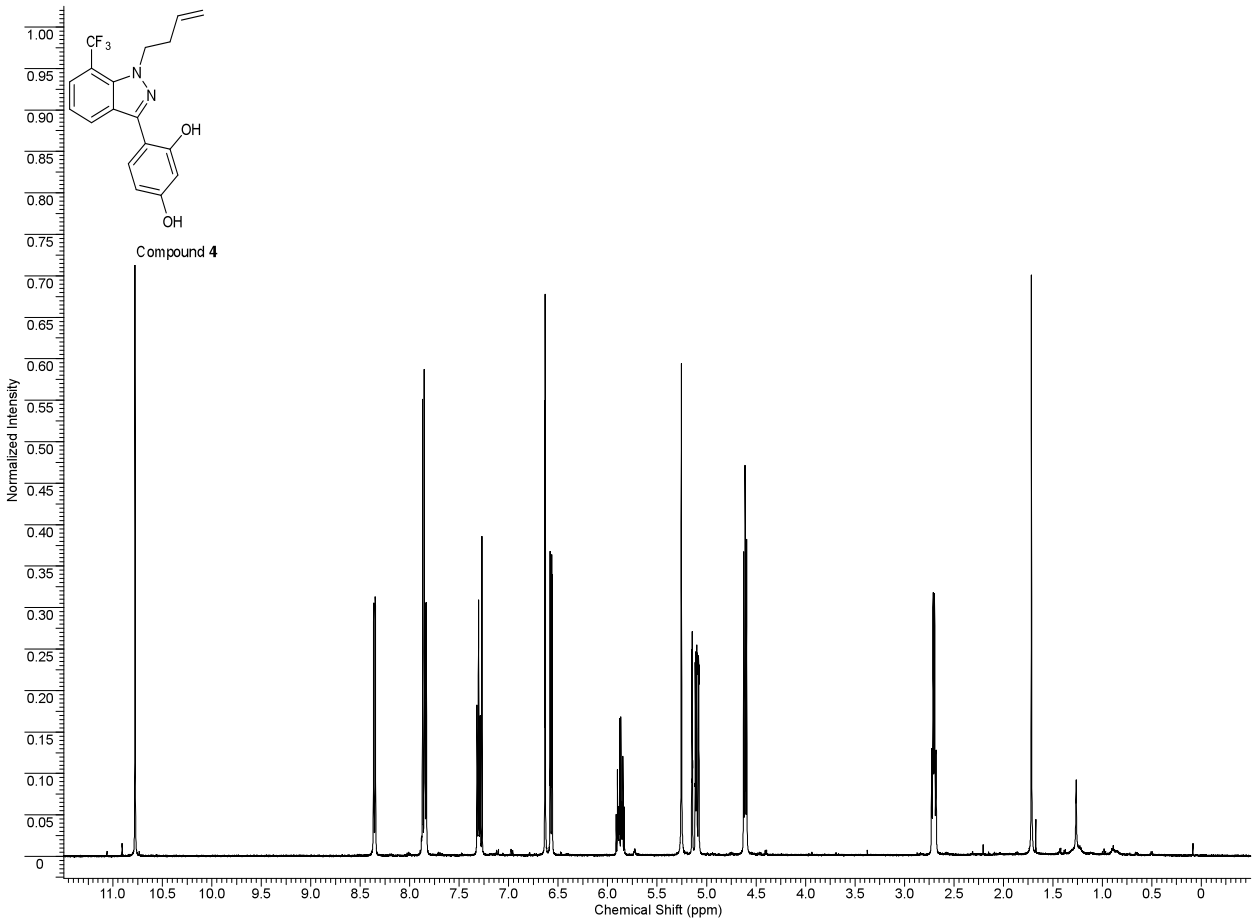


**Figure 3.** $^{1}$HNMR spectrum of compound **4**

**4-(1-(3-Methylbut-2-enyl)-7-(trifluoromethyl)-1H-indazol-3-yl)benzene-1,3-diol (5)**. Followed general procedure described above using 19 mg NaH (0.46 mmol) and 69 mg (0.46 mmol) of 1-bromo-3-methyl-2-butene stirred at room temperature for 4 h. Flash column eluted with 25–50% EtOAc in hexanes gave 54 mg (48%) of **5**. $^{1}$H NMR (500 MHz, $CDCl_3$) δ 1.78 (s, 3 H), 1.88 (s, 3 H), 4.94 (s, 1 H), 5.14 (d, *J*=6.84 Hz, 2 H), 5.45 (t, *J*=6.84 Hz, 1 H), 6.55 (dd, *J*=8.42, 2.56 Hz, 1 H), 6.60 (d, *J*=2.44 Hz, 1 H), 7.30 (t, *J*=7.93 Hz, 1 H), 7.84 (d, *J*=7.32 Hz, 1 H), 7.88 (d, *J*=8.55 Hz, 1 H), 8.37 (d, *J*=8.30 Hz, 1 H), 10.90 (s, 1 H). $^{13}$C NMR (500 MHz, $CDCl_3$) δ 25.9, 29.9, 49.3 (d, *J*=4.60 Hz), 104.2, 107.4, 110.7, 119.0, 120.2, 124.1, 126.4, 126.4 (d, *J*=6.44 Hz), 128.4, 137.6, 143.9, 157.1, 158.1. HRMS (ESI$^+$) *m/z* calcd for $C_{19}H_{18}N_2O_2F_3^+$ 363.1320, found 363.1317.

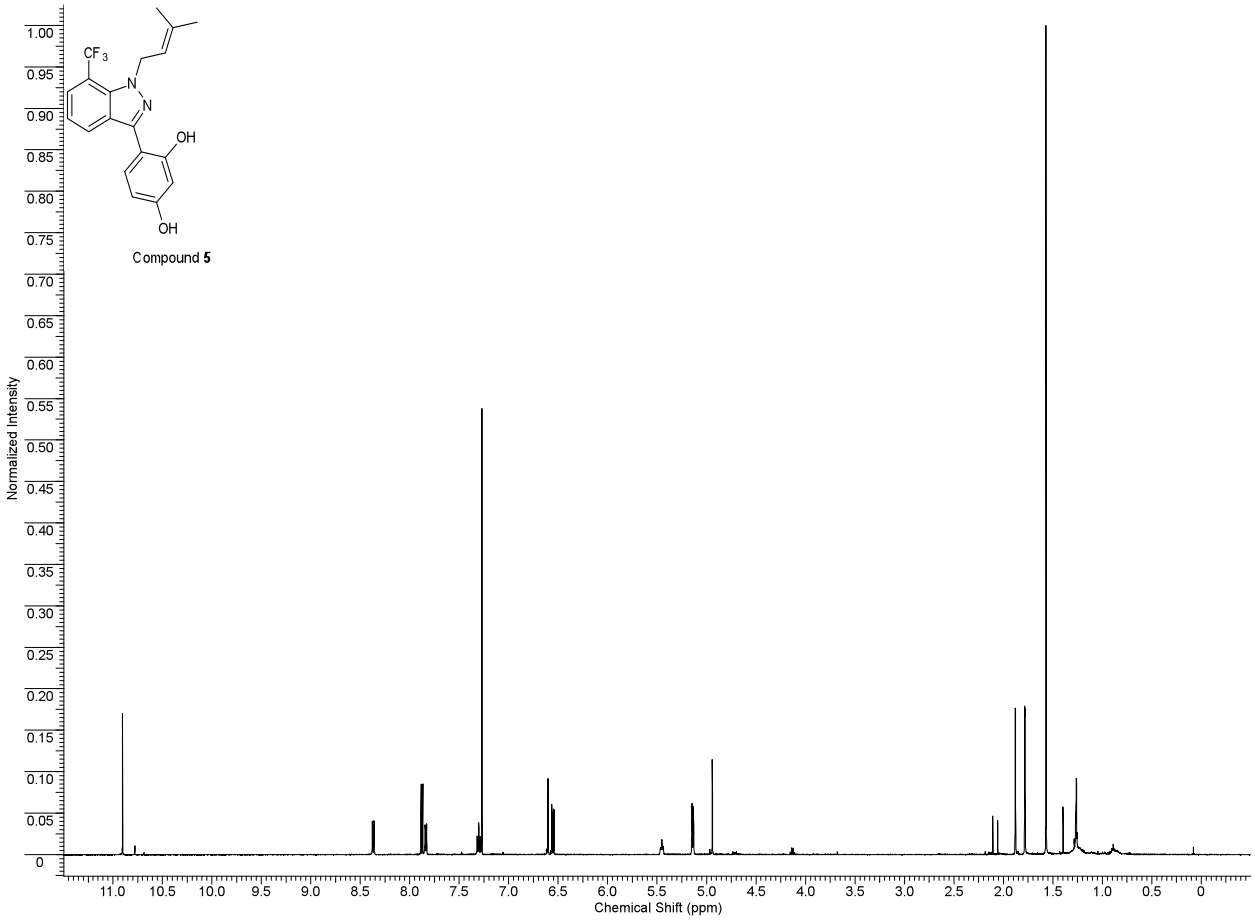


**Figure 4.** $^{1}$HNMR spectrum of compound **5**

**4-(1-Benzyl-7-(trifluoromethyl)-1H-indazol-3-yl)benzene-1,3-diol (6)**. Followed general procedure described above using 20 mg NaH (0.50 mmol) and 58 mg (0.34 mmol) of benzyl bromide stirred at room temperature for 24 h. Flash column eluted with 25–50% EtOAc in hexanes gave 38 mg (32%) of **6**. $^{1}$H NMR (500 MHz, $CDCl_3$) δ 5.13 (s, 1 H), 5.78 (s, 2 H), 6.55 (d, *J*=2.44 Hz, 1 H), 6.57 (q, *J*=2.28 Hz, 1 H), 7.14 (d, *J*=6.59 Hz, 2 H), 7.26 - 7.36 (m, 4 H), 7.86 (d, *J*=7.32 Hz, 1 H), 7.88 (d, *J*=8.06 Hz, 1 H), 8.40 (d, *J*=8.30 Hz, 1 H), 10.59 (s, 1 H). $^{13}$C NMR (500 MHz, $CDCl_3$) δ 54.9 (d, *J*=4.88 Hz), 104.3, 107.6, 110.4, 120.6, 124.3, 126.8 (d, *J*=6.84 Hz), 127.1, 127.2, 128.0, 128.6, 128.9, 136.3, 136.8, 144.5, 157.3, 158.0. HRMS (ESI$^+$) *m/z* calcd for $C_{21}H_{16}N_2O_2F_3^+$ 385.1164, found 385.1182.

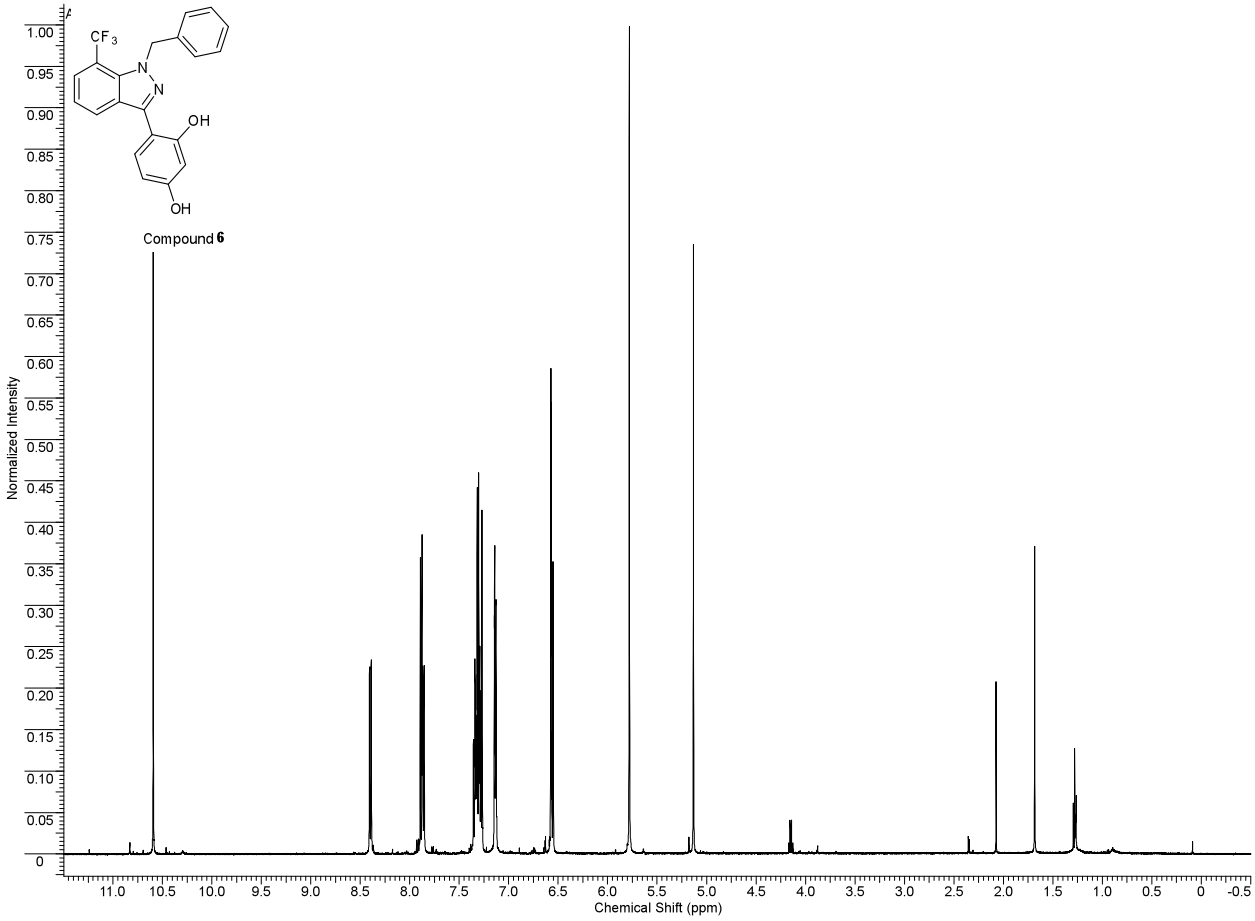


**Figure 5.** $^{1}$HNMR spectrum of compound **6**

**4-(1-Isobutyl-7-(trifluoromethyl)-1H-indazol-3-yl)benzene-1,3-diol (7)**. Followed general procedure described above using 28 mg NaH (0.70 mmol) and 94 mg (0.69 mmol) of isobutyl bromide stirred at 50 °C for 24 h. Flash column eluted with 25–50% EtOAc in hexanes gave 34 mg (31%) of **7**. $^{1}$H NMR (500 MHz, $CDCl_3$) δ 0.96 (d, *J*=6.59 Hz, 6 H), 2.42 (septet, *J*=7.08 Hz, 1 H), 4.35 (d, *J*=7.32 Hz, 2 H), 5.34 (s, 1 H), 6.58 (dd, *J*=8.42, 2.56 Hz, 1 H), 6.63 (s, 1 H), 7.30 (t, *J*=7.81 Hz, 1 H), 7.84 (d, *J*=7.32 Hz, 1 H), 7.88 (d, *J*=8.55 Hz, 1 H), 8.37 (d, *J*=8.30 Hz, 1 H), 10.96 (s, 1 H). $^{13}$C NMR (500 MHz, $CDCl_3$) δ 20.2, 29.7, 58.1 (d, *J*=3.91 Hz), 104.3, 107.6, 110.0, 110.5, 120.2, 123.9, 126.6 (d, *J*=6.84 Hz), 126.9, 128.4, 143.7, 157.2, 158.0. HRMS (ESI$^+$) *m/z* calcd for $C_{18}H_{18}N_2O_2F_3^+$ 351.1320, found 351.1315.

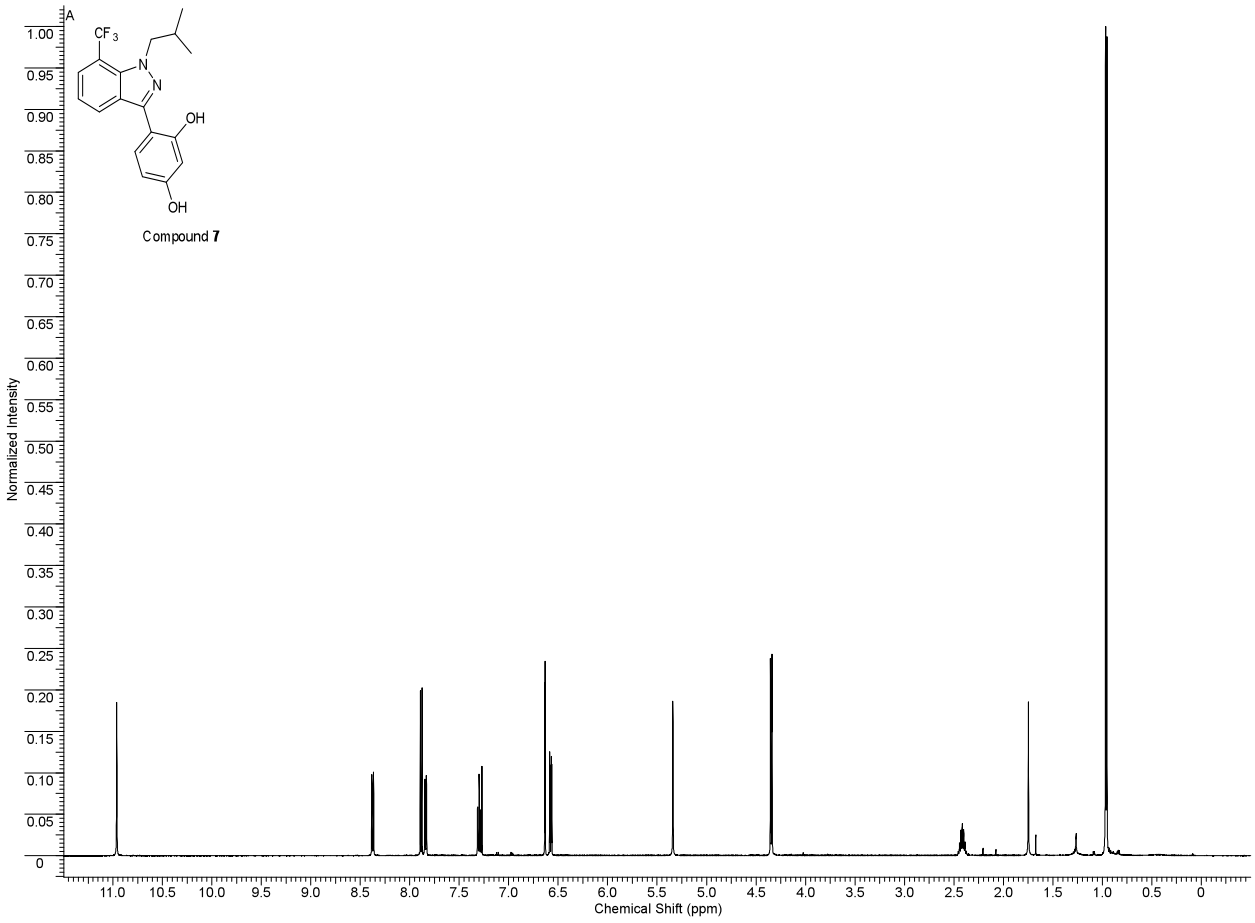


**Figure 6.** $^{1}$HNMR spectrum of compound **7**

**References**

Konieczny, M.T., Maciejewski, G., and Konieczny, W. (2005). Selectivity adjustment in the cleavage of allyl phenyl and methyl phenyl ethers with boron trifluoride-methyl sulfide complex. Synthesis, 1575-1577.

Mosyak, L., Xu, Z.B., Stahl, M., Hum, W.-T., Somers, W.S., and Manas, E.S. (2006). Crystal structure of estrogen receptor alpha bound to synthetic ligands in drug design (Application: US, (Wyeth, USA).), pp. 127 pp.

Steffan, R.J., Matelan, E., Ashwell, M.A., Moore, W.J., Solvibile, W.R., Trybulski, E., Chadwick, C.C., Chippari, S., Kenney, T., Eckert, A.*, et al.* (2004). Synthesis and Activity of Substituted 4-(Indazol-3-yl)phenols as Pathway-Selective Estrogen Receptor Ligands Useful in the Treatment of Rheumatoid Arthritis. J Med Chem *47*, 6435-6438.